

Article

# Synthesis and Characterization of Ag-Ag<sub>2</sub>O/TiO<sub>2</sub>@polypyrrole Heterojunction for Enhanced Photocatalytic Degradation of Methylene Blue

Rajeev Kumar <sup>1</sup>, Reda M. El-Shishtawy <sup>2,3</sup> and Mohamed A. Barakat <sup>1,4,\*</sup>

<sup>1</sup> Department of Environmental Sciences, Faculty of Meteorology, Environment, and Arid Land Agriculture, King Abdulaziz University, Jeddah 21589, Saudi Arabia; olifiaraju@gmail.com

<sup>2</sup> Chemistry Department, Faculty of Science, King Abdulaziz University, P.O. Box 80203, Jeddah, Saudi Arabia; elshishtawy@hotmail.com

<sup>3</sup> Dyeing, Printing and Textile Auxiliaries Department, Textile Research Division, National Research Center, Dokki, Giza 12311, Egypt

<sup>4</sup> Central Metallurgical R & D Institute, Helwan 11421, Cairo, Egypt

\* Correspondence: mabarakat@gmail.com; Tel.: +966-2-640-0000 (ext. 64821); Fax: +966-2-695-2364

Academic Editor: Dionysios (Dion) D. Dionysiou

Received: 30 March 2016; Accepted: 17 May 2016; Published: 25 May 2016

**Abstract:** Hybrid multi-functional nanomaterials comprising two or more disparate materials have become a powerful approach to obtain advanced materials for environmental remediation applications. In this work, an Ag-Ag<sub>2</sub>O/TiO<sub>2</sub>@polypyrrole (Ag/TiO<sub>2</sub>@PPy) heterojunction has been synthesized by assembling a self-stabilized Ag-Ag<sub>2</sub>O (*p* type) semiconductor (denoted as Ag) and polypyrrole ( $\pi$ -conjugated polymer) on the surface of rutile TiO<sub>2</sub> (*n* type). Ag/TiO<sub>2</sub>@PPy was synthesized through simultaneous oxidation of pyrrole monomers and reduction of AgNO<sub>3</sub> in an aqueous solution containing well-dispersed TiO<sub>2</sub> particles. Thus synthesized Ag/TiO<sub>2</sub>@PPy was characterized using X-ray diffraction (XRD), X-ray photoelectron spectroscopy (XPS), field emission scanning electron microscopy (FE-SEM), transmission electron microscopy (TEM), and UV-Vis diffuse reflectance spectroscopy (UV-vis DSR). The photocatalytic activity of synthesized heterojunction was investigated for the decomposition of methylene blue (MB) dye under UV and visible light irradiation. The results revealed that  $\pi$ -conjugated *p-n* heterojunction formed in the case of Ag/TiO<sub>2</sub>@PPy significantly enhanced the photodecomposition of MB compared to the *p-n* type Ag/TiO<sub>2</sub> and TiO<sub>2</sub>@PPy (*n- $\pi$* ) heterojunctions. A synergistic effect between Ag-Ag<sub>2</sub>O and PPy leads to higher photostability and a better electron/hole separation leads to an enhanced photocatalytic activity of Ag/TiO<sub>2</sub>@PPy under both UV and visible light irradiations.

**Keywords:** Ag-Ag<sub>2</sub>O/TiO<sub>2</sub>@polypyrrole heterojunction; photocatalysis; methylene blue; Degradation mechanism

## 1. Introduction

Heterogeneous photocatalytic degradation of pollutants by an *n*-type semiconductor, *i.e.*, TiO<sub>2</sub> nanoparticles, has been widely studied in the last decade [1]. Rutile and anatase polymorphs of TiO<sub>2</sub> are the most studied structures, among which anatase shows much higher photocatalytic activity [2]. Meanwhile, rutile TiO<sub>2</sub> has low band-gap energy (~3.02 eV) compared to anatase TiO<sub>2</sub> (~3.2), which allows it to absorb solar energy more efficiently than the anatase form, hence making it a suitable candidate for photocatalytic applications. However, the wide band gap of rutile TiO<sub>2</sub> and poor quantum yield results in low photo efficiency, which limits its use in visible light [2,3]. In order to

extend the photo response in visible light and improve the photocatalytic activity of  $\text{TiO}_2$ , various doping, co-doping, composite, coupling, *etc.* techniques have been investigated and various materials with  $\text{TiO}_2$  such as carbon [4], Pt(II) [5],  $\text{CoFe}_2\text{O}_4$  [6], N, Fe, Fe-N [7], Ag-polyaniline [8], *etc.* have gained much attention in the recent past. Among these, noble metals such as Au, Ag, Pt, *etc.* have shown high photocatalytic enhancing property by inhibiting charge carrier recombination within the semiconductor materials [9]. Silver ( $\text{Ag}^0/\text{Ag}^+$ ) is one of the most promising noble metals used to make visible light photoactive materials.  $\text{Ag}_2\text{O}$  is a *p*-type semiconductor with energy  $\sim 1.46$  eV and has been widely used as photocatalyst in single, binary, or multiple composite systems [10,11]. Under UV light irradiation,  $\text{Ag}_2\text{O}$  behaves as an effective  $e^-$ -absorbing agent, while under visible light irradiation it acts as an efficient photosensitizer [10,11]. However,  $\text{Ag}_2\text{O}$  is photosensitive but its instability under light irradiation ( $\text{Ag}_2\text{O} \rightarrow 2\text{Ag} + 1/2\text{O}_2$ ) is the main problem associated with its photocatalytic uses. Wang *et al.* [10] reported that  $\text{Ag}_2\text{O}$  shows higher stability in the presence of metallic Ag. In an Ag- $\text{Ag}_2\text{O}$  system, Ag acts as an electron scavenger, which prevents the reduction of  $\text{Ag}_2\text{O}$ . Therefore, the Ag- $\text{Ag}_2\text{O}$  system may be an effective methodology to overcome stability problems [8,12]. Moreover, the Ag- $\text{Ag}_2\text{O}$  system may enhance photocatalytic activity, increase the lifetime of the photocatalyst, and inhibit the leaching and aggregation of nano-sized semiconductor particles into the water [7,13].

Recently, conducting polymers such as polypyrrole (PPy), polythiophene, and polyaniline have been used as photosensitizers to modify the photocatalyst semiconductors band. These polymers can efficiently donate electrons, act as hole transporters, have good interfacial electron transfer process, and prevent oxidation/reduction of metallic nanoparticles under visible light excitation [14,15]. Among these conducting polymers, PPy possesses high electrochemical reversibility, superior conductivity, and high polarizability, and can also be easily synthesized by electrochemical or chemical routes [14,16]. In addition, the high thermal and chemical stability of PPy makes it a promising material and a stable photosensitizer, which may enhance the photocatalytic activity of  $\text{TiO}_2$  [17]. Various reports on the photocatalytic applications of PPy-based materials such as AgCl/PPy, [18], PPy- $\text{TiO}_2$ -Fly ash [19], PPy/ $\text{Bi}_2\text{WO}_6$  [12], *etc.* have shown high photocatalytic efficiency in visible light for the degradation of organic pollutants.

On the basis of the aforementioned considerations, it may be assumed that a multi-component nanocomposite of Ag- $\text{Ag}_2\text{O}$ , polypyrrole (PPy) and  $\text{TiO}_2$  would possess a narrow band gap and higher photocatalytic activity and thus might be successfully applied for visible light photocatalysis. Therefore, in this work, an Ag/ $\text{TiO}_2$ @PPy nanocomposite was synthesized and characterized by various techniques. The photocatalytic activity of the as-synthesized nanocomposite was evaluated for the degradation of methylene blue (MB) in an aqueous solution under UV and visible light irradiation. The photocatalytic activity of Ag/ $\text{TiO}_2$ @PPy was also compared with two component composites *i.e.*, Ag/ $\text{TiO}_2$  and  $\text{TiO}_2$ @PPy.

In this work, an aqueous medium was used for the synthesis of a self-stabilized Ag- $\text{Ag}_2\text{O}$  structure in the presence of pyrrole. In this synthesis, pyrrole acts as a reducing agent and undergoes oxidative polymerization in the presence of  $\text{Ag}^+$  in aquatic conditions. This reaction was conducted in the homogeneous  $\text{TiO}_2$  suspension to deposit Ag- $\text{Ag}_2\text{O}$  and PPy over the  $\text{TiO}_2$  surface. The main objective of this work is to stabilize and enhance the photocatalytic activity of  $\text{Ag}_2\text{O}$  under solar irradiation.  $\text{Ag}_2\text{O}$ , when photo-reduced to AgO, is unstable at room temperature and forms  $\text{Ag}^0$  and  $\text{O}_2$  ( $\text{Ag}_2\text{O} \rightarrow \text{AgO} + \text{Ag}$ ,  $\text{AgO} \rightarrow \text{Ag} + 1/2\text{O}_2$ ) [10]. Under light irradiation, photo-generated electrons and holes from the conduction band (CB) and valence band (VB) band of  $\text{Ag}_2\text{O}$ , respectively, reduce  $\text{Ag}^+$  ions into metallic Ag and oxidize lattice  $\text{O}^{2-}$  to  $\text{O}_2$ . For the stabilization of  $\text{Ag}_2\text{O}$ , the photo-generated electron and holes in  $\text{Ag}_2\text{O}$  must be separated immediately before lattice  $\text{O}^{2-}$  oxidation and lattice  $\text{Ag}^+$  reduction. For this purpose, simultaneous synthesis of Ag- $\text{Ag}_2\text{O}$ -PPy onto  $\text{TiO}_2$  has been done to stabilize and enhance the photocatalytic activity of  $\text{Ag}_2\text{O}$ .

## 2. Results and Discussion

In this hybrid system, metallic Ag collects and channels the photo-generated electrons from  $\text{Ag}_2\text{O}/\text{TiO}_2$  while PPy is assumed to transfer photo-generated holes to the solid–solution interface [10,20]. To confirm the existence of Ag– $\text{Ag}_2\text{O}$  and PPy in the Ag/ $\text{TiO}_2$ @PPy heterostructure, XPS analysis was performed as shown in Figure 1. The high-resolution spectra for Ag 3d demonstrate that silver is present in more than one oxidation state. The peaks appearing at 367.63 and 373.65 eV correspond to the Ag  $3d_{5/2}$  and Ag  $3d_{3/2}$ , respectively, representing silver in  $\text{Ag}^+$  ( $\text{Ag}_2\text{O}$ ) oxidation state. The other peaks of Ag  $3d_{5/2}$  and Ag  $3d_{3/2}$  peaks at 368.1 and 374.11 eV, respectively, with a separation of 6 eV, confirm the existence of silver in the  $\text{Ag}^0$  state. These binding energies values are in good agreement with the reported values for  $\text{Ag}^0$  and  $\text{Ag}_2\text{O}$  [10,21,22]. The binding energies for 1 Os peaks located at 530.1, 531.66 and 533.84 eV are ascribed to the  $\text{O}^{2-}$  in  $\text{TiO}_2$  and  $\text{Ag}_2\text{O}$ , respectively [22,23]. The characteristic peaks ( $\text{Ti}^{4+}$ ) of Ti  $2p_{3/2}$  and  $2p_{1/2}$  appeared at 458.84 and 464.68 eV, respectively [22]. The C 1s peaks of PPy, corresponding to the binding energies at 285 and 286.09 eV, can be attributed to the C–C and C–N groups and the other C 1s peak at 289.05 eV is attributed to the electronic transition on PPy ring [24]. The characteristic spectrum of pyrrolylium nitrogen ( $-\text{NH}-$ ) as N 1s' single major component appears at 399.7 eV, while the N 1s peak in our case appeared at low binding energy *i.e.*, at 397.38 eV, which may be due to the dehydrogenation of pyrrolylium nitrogen [25,26].

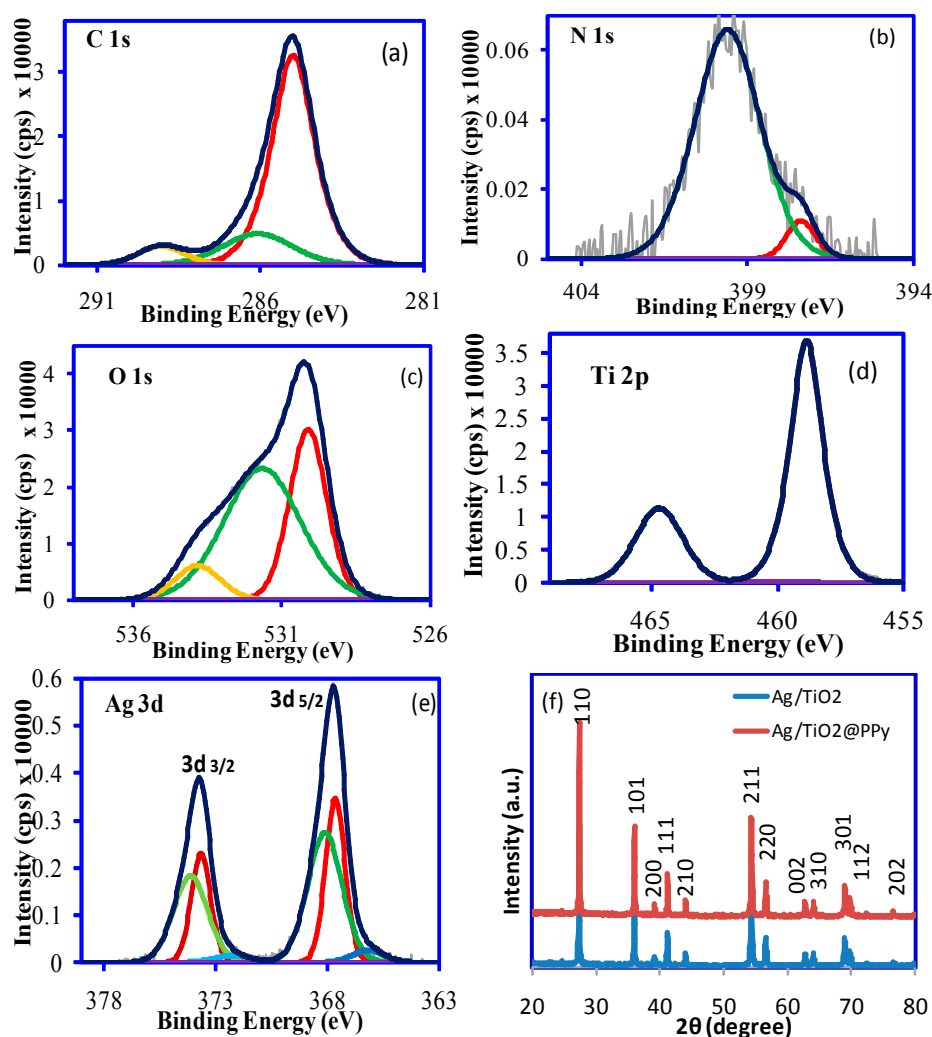
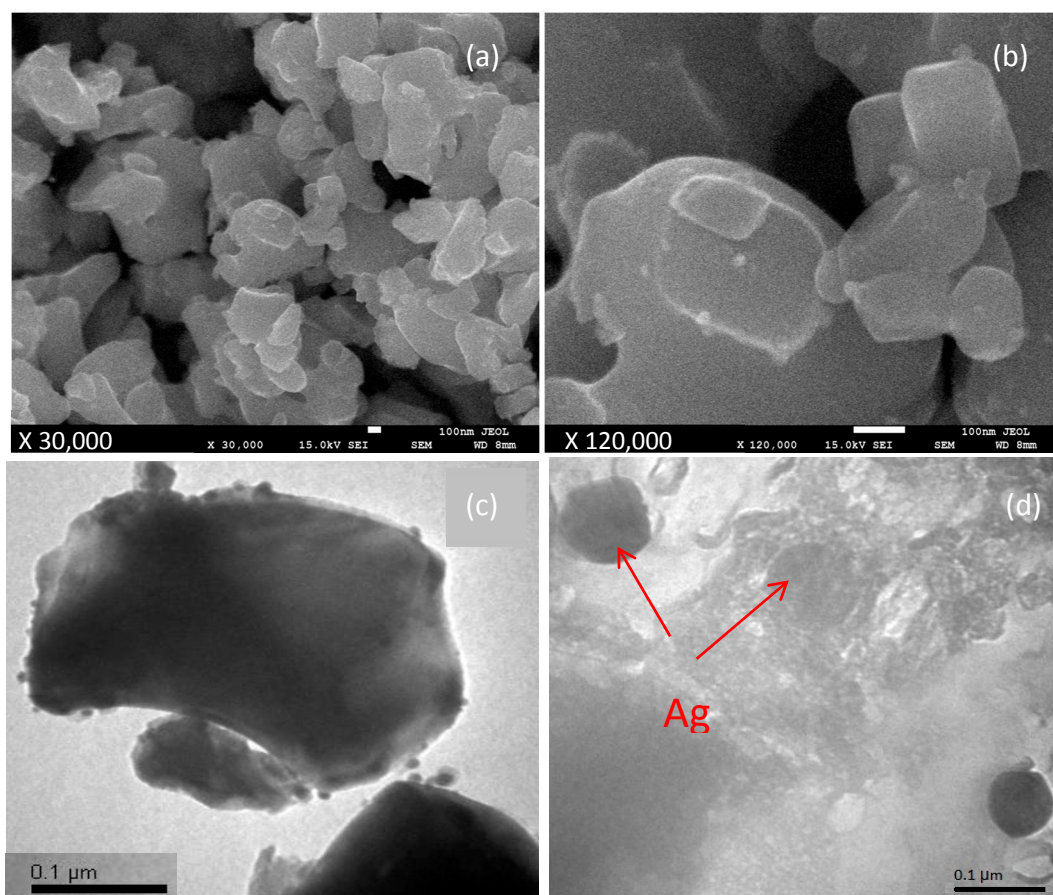


Figure 1. XPS analysis of Ag/ $\text{TiO}_2$ @PPy (a–e) and XRD patterns of Ag/ $\text{TiO}_2$  and Ag/ $\text{TiO}_2$ @PPy (f).

XRD spectra of Ag/TiO<sub>2</sub> and Ag/TiO<sub>2</sub>@PPy heteroconjugation are shown in Figure 1f. The XRD analysis showed highly crystalline rutile phase of TiO<sub>2</sub> (JCPDS card No. 01-071-0650) without other detectable impurities, suggesting that the presence of Ag<sub>2</sub>O-Ag and PPy did not change the lattice structure of TiO<sub>2</sub>. However, the peaks for Ag<sub>2</sub>O-Ag and PPy are not observed due to its low concentration. Similar explanations have also been reported by several other researchers for indistinct XRD peaks in their respective composite systems [27,28]. The crystallite size of Ag/TiO<sub>2</sub> and Ag/TiO<sub>2</sub>@PPy hybrid structures were found to be in the ranges of 34.3–61.9 nm and 61.3–80.8 nm, respectively.

To study the surface morphology and presence of Ag in Ag/TiO<sub>2</sub>@PPy nanocomposite, SEM and TEM analysis were performed as shown in Figure 2. The SEM image (Figure 2a) shows the highly irregular shape of the nanocomposite with large globules of different sizes. A thorough examination at higher magnification (Figure 2b) clearly shows Ag particles deposited on the TiO<sub>2</sub>@PPy polymer system. The TEM images of Ag/TiO<sub>2</sub>@PPy (Figure 2c,d) clearly demonstrate that spherical Ag nanoparticles are immobilized on the PPy-coated TiO<sub>2</sub>, hence confirming the successful synthesis of an Ag/TiO<sub>2</sub>@PPy hybrid material.



**Figure 2.** Surface morphology of Ag/TiO<sub>2</sub>@PPy composite, SEM images (a,b) and TEM (c,d).

The optical properties of Ag/TiO<sub>2</sub>, TiO<sub>2</sub>@PPy, and Ag/TiO<sub>2</sub>@PPy were studied by UV-visible diffusion reflectance spectroscopy and the spectra are shown in Figure 3. All the studied composites exhibit the sharp adsorption edge < 400 nm, indicating the strong light absorption capability in both UV and visible light ranges. The absorption band in the UV region *i.e.*, >380 nm is the characteristic band of Ti-O [29]. The spectrum of TiO<sub>2</sub>@PPy and Ag/TiO<sub>2</sub>@PPy is above Ag/TiO<sub>2</sub>, which can be attributed to the  $\pi$ - $\pi^*$  transition of the polypyrrole backbone. The optical band gaps of Ag/TiO<sub>2</sub>,

TiO<sub>2</sub>/PPy, and Ag/TiO<sub>2</sub>/PPy are 2.97, 2.89, and 2.91 eV, respectively. As observed from the band gap analysis, the incorporation of Ag and PPy onto TiO<sub>2</sub> significantly narrowed the band gap energy. Therefore, the UV and visible light response of the hybrid materials improved, which will result in enhanced photocatalytic properties.

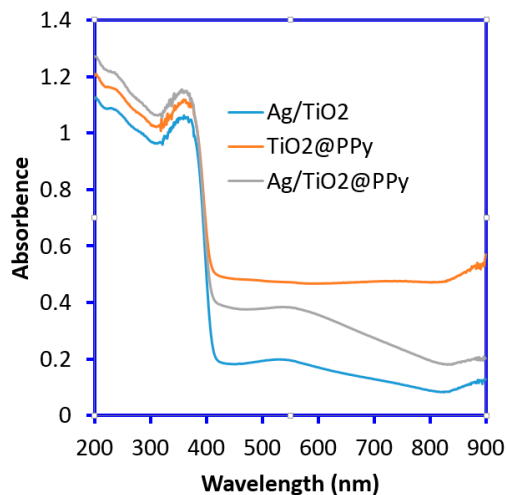


Figure 3. UV-vis spectra of Ag/TiO<sub>2</sub>, TiO<sub>2</sub>@PPy, and Ag/TiO<sub>2</sub>@PPy heterostructures.

The photocatalytic activity of Ag/TiO<sub>2</sub>@PPy heterostructure was comparatively studied with Ag/TiO<sub>2</sub> and TiO<sub>2</sub>@PPy by using MB as a model pollutant in aqueous solution under UV and visible light irradiation. The degradation of MB as a function of irradiation time is shown in Figure 4. From Figure 4, it can be seen that the degradation of MB in UV irradiation was higher compared to the visible light irradiation and the photocatalytic behavior followed the order: TiO<sub>2</sub> < TiO<sub>2</sub>@PPy < Ag/TiO<sub>2</sub> < Ag/TiO<sub>2</sub>@PPy. The observed higher photocatalytic activity of Ag/TiO<sub>2</sub>@PPy than TiO<sub>2</sub>@PPy, Ag/TiO<sub>2</sub>, and TiO<sub>2</sub> may be due to the fact that PPy and Ag nanoparticles may act as an interfacial charge carrier in the Ag-TiO<sub>2</sub>-PPy system, which leads to the prevention of electron-hole (e<sup>-</sup>/h<sup>+</sup>) pair recombination, thereby increasing the photocatalytic activity. Moreover, the effectiveness of a ternary composite system (Ag/TiO<sub>2</sub>@PPy) was comparatively enhanced due to the synergistic effect of Ag (Ag-Ag<sub>2</sub>O), TiO<sub>2</sub> and PPy [29,30]. On the basis of this study, the Ag/TiO<sub>2</sub>@PPy composite was used for further photocatalytic studies.

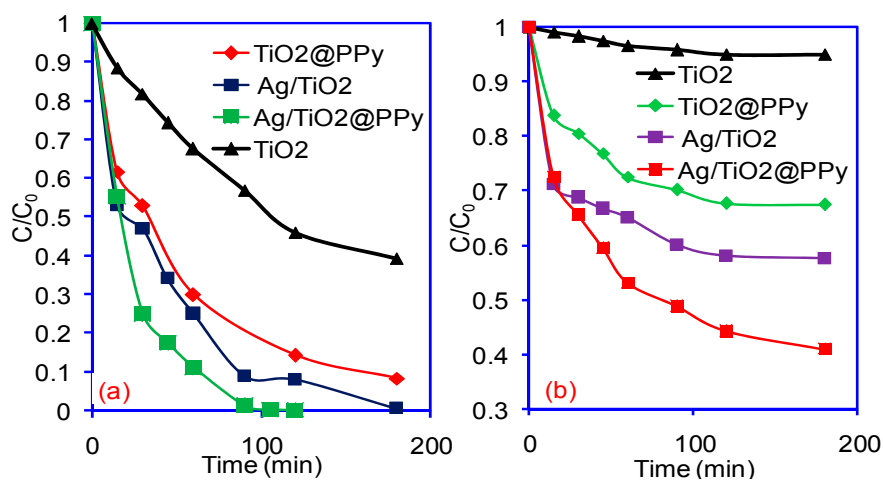
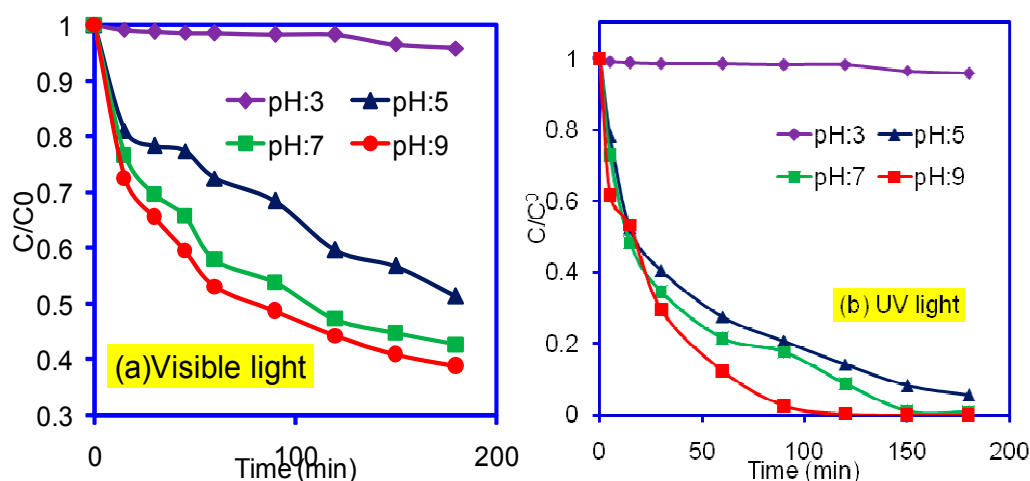


Figure 4. Comparison of MB photocatalytic degradation efficiency of synthesized heterojunctions under (a) UV and (b) visible light irradiation.

The solution pH plays an important role in the interaction of a dye with the photocatalyst surface and their degradation. The UV and visible light photocatalytic activity of Ag/TiO<sub>2</sub>@PPy as a function of initial dye solution pH are shown in Figure 5. The degradation of MB is strongly affected by the solution pH and it increased with the increase in the solution pH from 3.0 to 9.0. The maximum degradation was observed at pH 9.0 for both UV and visible light. The observed behavior could be explained on the basis of surface charge on the Ag/TiO<sub>2</sub>@PPy at different solution pH values. Lower degradation efficiency of Ag/TiO<sub>2</sub>@PPy for MB in acidic solution was due to protonation of Ag/TiO<sub>2</sub>@PPy (NH<sub>2</sub><sup>+</sup> in PPy), which generates a positive surface charge and shows electrostatic repulsion with the positively charged MB ions [31,32]. As the solution pH increases from acidic to alkaline, the surface charge starts to turn negative and degradation of MB increases. At pH 9.0, deprotonation of nitrogen atoms of PPy takes place and the surface of Ag/TiO<sub>2</sub>@PPy becomes negatively charged, which interacts with cationic MB ions electrostatically, resulting in an enhancement of the photocatalytic degradation of MB [31,33]. Besides electrostatic forces,  $\pi$ - $\pi$  stacking, hydrogen bonding, and van der Waals forces are also expected to be involved in the interaction of MB with Ag/TiO<sub>2</sub>@PPy. Due to these forces, reasonable photocatalytic degradation of MB was observed at pH 5.0 and 7.0.



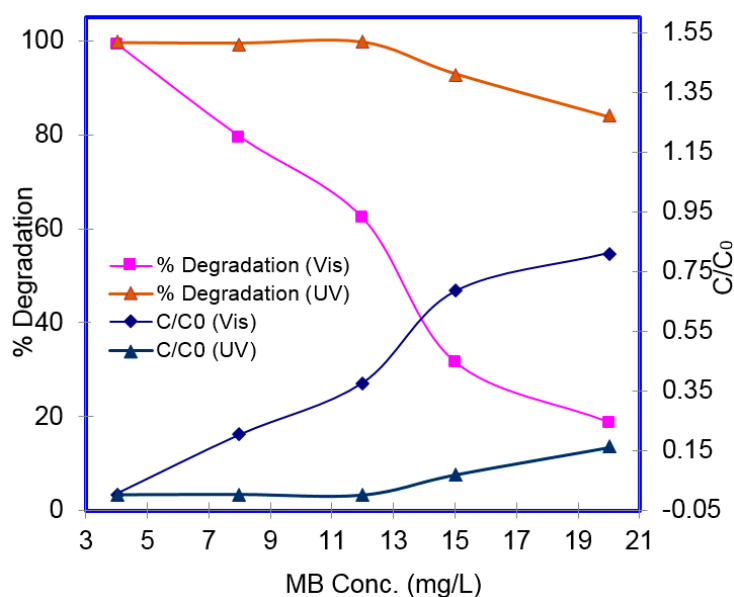
**Figure 5.** Effect of solution pH on MB photodecomposition using Ag/TiO<sub>2</sub>@PPy heterostructure under UV and visible light irradiation.

The rate constant for MB degradation was calculated using a first-order reaction kinetic model:  $\ln(C/C_0) = -kt$ . where  $C_0$  and  $C$  denotes the concentration of MB before and after photocatalysis, respectively; and  $k$  and  $t$  are the rate constant and irradiation time, respectively. The values of rate constant calculated from the linear relation of  $\ln(C/C_0)$  vs.  $t$  are mentioned in Table 1. It can be seen from Table 1 that the rate constant values increased with the increase in the solution pH, confirming that a higher pH was favorable for MB degradation in an aqueous solution. Hence, the efficiency of Ag/TiO<sub>2</sub>@PPy under UV irradiation was much higher than the visible light photocatalytic degradation of MB. These results are in agreement with the abovementioned data. The higher efficacy of Ag/TiO<sub>2</sub>@PPy under UV light irradiation is due to the higher photon absorption by all three components (Ag, TiO<sub>2</sub>, and PPy) while in visible light irradiation only Ag and PPy can be photo-excited [11].

**Table 1.** First order rate constants for the degradation of MB using Ag/TiO<sub>2</sub>@PPy.

| pH | $k$ (UV) (min <sup>-1</sup> ) | $R^2$ | $k$ (Visible) (min <sup>-1</sup> ) | $R^2$ |
|----|-------------------------------|-------|------------------------------------|-------|
| 3  | 0.000                         | 0.834 | 0.000                              | 0.488 |
| 5  | 0.014                         | 0.987 | 0.002                              | 0.987 |
| 7  | 0.024                         | 0.929 | 0.003                              | 0.955 |
| 9  | 0.044                         | 0.968 | 0.003                              | 0.947 |

The effect of initial MB concentration in aquatic solution was studied in the range of 4 to 20 mg/L, as depicted in Figure 6. At lower concentrations almost 100% degradation of MB was observed under UV and visible light irradiation. As the concentration of MB increased from 4 to 20 mg/L, the degradation efficiency decreased from 99.62% to 83.9% under UV irradiation, while in visible light the efficiency decreased from 99.37% to 18.85%. The reduction in the degradation rate of MB can be explained on the basis of the higher surface coverage of Ag/TiO<sub>2</sub>@PPy with MB ions, which suppressed the production of •OH radicals [34]. Moreover, the increase in the optical density of the MB solution as a consequence of increasing the concentration of MB results in a decrease in the light penetration in the solution. Therefore, fewer photons reach the Ag/TiO<sub>2</sub>@PPy surface due to the UV/visible light screening effect of MB itself. This effect reduces the generation of O<sub>2</sub>•<sup>-</sup> and •OH, which causes a decrease in the efficiency of the photocatalytic reaction [34,35].

**Figure 6.** Effect of initial dye concentration on MB photocatalytic degradation.

The aforementioned results confirmed that a  $\pi$ -conjugated Ag/TiO<sub>2</sub>@PPy heterojunction photocatalyst has higher photocatalytic activity than Ag/TiO<sub>2</sub> and TiO<sub>2</sub>@PPy under both UV and visible light irradiation. A schematic illustration for e<sup>-</sup>/h<sup>+</sup> separation in Ag/TiO<sub>2</sub>@PPy heterojunction under UV and visible light irradiation have been shown in Figure 7. Under UV light irradiation, both Ag<sub>2</sub>O (Ag<sub>2</sub>O + h $\nu$  → h<sup>+</sup> + e<sup>-</sup>) and TiO<sub>2</sub> (TiO<sub>2</sub> + h $\nu$  → h<sup>+</sup> + e<sup>-</sup>) could be photo-excited to generate e<sup>-</sup> and h<sup>+</sup> pairs, while under visible light Ag<sub>2</sub>O and PPy (PPy + h $\nu$  → h<sup>+</sup> + e<sup>-</sup>) [36] get excited due to the narrow band gap (1.3 eV and 2.5 eV), thereby producing e<sup>-</sup> and h<sup>+</sup> pairs. The CB level of Ag<sub>2</sub>O has a higher positive potential (+0.2 eV *vs.* SHE) compared with the single electron reduction of O<sub>2</sub> (-0.046 V *vs.* SHE). Therefore, photogenerated e<sup>-</sup> from Ag<sub>2</sub>O can be transferred by metallic Ag (Ag<sup>+</sup>/Ag: 0.7991 V, *vs.* SHE) to the O<sub>2</sub> and thereby generate O<sub>2</sub>•<sup>-</sup> and •OH radicals (e<sup>-</sup> + O<sub>2</sub> + H<sub>2</sub>O → O<sub>2</sub>•<sup>-</sup> + •OH) through a chain of reactions [10,21]. In the combined system Ag/TiO<sub>2</sub>@PPy,  $\pi$

orbital becomes the highest occupied molecular orbital (HOMO) and the lowest occupied molecular orbital level (LUMO) of PPy is energetically higher than the CB edge of rutile  $\text{TiO}_2$  (3.0 eV) [9]. When PPy is harvested in visible light, the photogenerated  $e^-$  are transferred to the excited state and these  $e^-$  can be readily injected into the CB of  $\text{TiO}_2$  and photogenerated  $h^+$  channeled by the PPy to the solid solution interface, which generates hydroxyl radicals ( $h^+ + \text{H}_2\text{O} \rightarrow \cdot\text{OH} + \text{H}^+$ ). The photogenerated  $e^-$  trapped by the catalyst surface adsorbs  $\text{H}_2\text{O}$  and  $\text{O}_2$ , which produces superoxide radical anions ( $\text{O}_2^{\cdot-}$ ,  $\text{OOH}$ , and  $\text{OH}^-$ ), while photogenerated  $h^+$  reacts with  $\text{OH}^-$  and  $\text{H}_2\text{O}$  to generate  $\text{HO}\cdot$  and  $\text{H}^+$  species [37]. As a result,  $\text{Ag}/\text{TiO}_2@\text{PPy}$  had a fast charge separation and enhanced the life of  $e^-/h^+$  recombination, resulting in higher and faster photocatalytic activity.

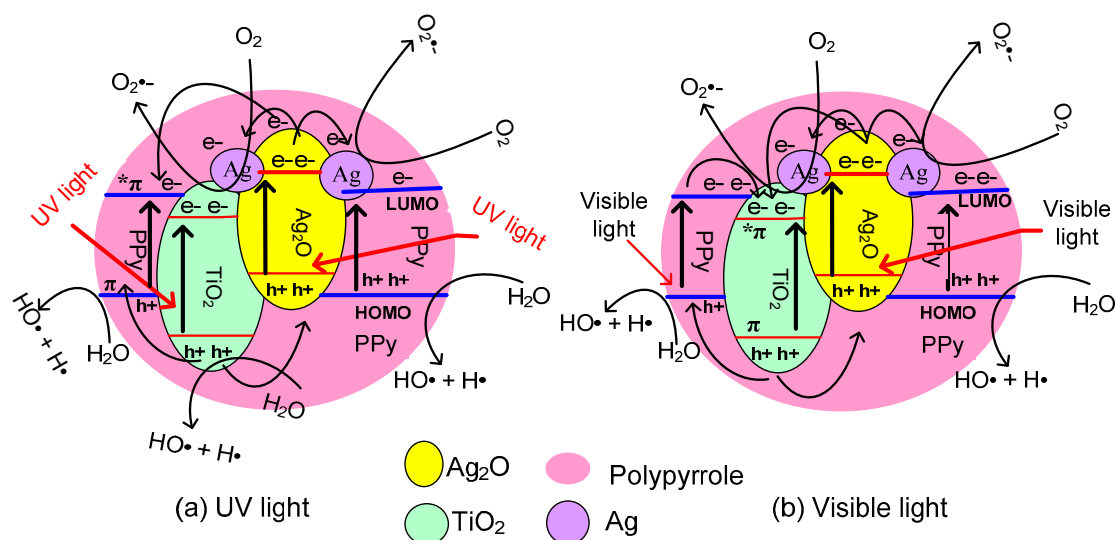


**Figure 7.** Schematic representation of possible electron/hole pair separation mechanism of the Ag-Ag<sub>2</sub>O/TiO<sub>2</sub>@PPy heterostructure under (a) UV and (b) visible light irradiation.

### 3. Materials and Methods

Titanium dioxide (rutile  $\text{TiO}_2$ ) from Alfa-Aesar (Beijing, China) was used as the photocatalyst support. Pyrrole and  $\text{AgNO}_3$  were purchased from Sigma-Aldrich (Taufkirchen, Germany), and used as received. Methylene blue (MB) [ $\text{C}_{16}\text{H}_{18}\text{N}_3\text{SCl}$ ] was purchased from Techno Pharma (Bahadurgarh, India). The aqueous solution of MB was prepared by dissolving 1 g of dye in 1 L solution and dilution was performed to get the desired concentration of MB for photocatalytic degradation studies.

#### 3.1. Synthesis of Ag/TiO<sub>2</sub> Nanocomposite

A mixture of rutile  $\text{TiO}_2$  (1.5 g) and 0.26 g  $\text{AgNO}_3$  (dissolved in 10 mL  $\text{H}_2\text{O}$ ) was mixed well and dried in an oven at 60 °C for 12 h. This mixture was then spread on the glass plate and placed under a UV lamp at a distance of 10 cm. Thereafter, the mixture was irradiated with 302 nm light source at room temperature for 6 h with occasional mixing to ensure homogeneity.

#### 3.2. Synthesis of TiO<sub>2</sub>@PPy and Ag/TiO<sub>2</sub>@PPy Nanocomposite

For the synthesis of  $\text{TiO}_2@\text{PPy}$ , first 1.5 g of rutile  $\text{TiO}_2$  was dispersed in 14 mL  $\text{H}_2\text{O}$  at room temperature, to which 0.26 g  $\text{AgNO}_3$  (dissolved in 10 mL  $\text{H}_2\text{O}$ ) and 6 mL pyrrole solution was added and thereafter the entire system was put under stirring conditions. To the above dispersion of pyrrole,  $\text{AgNO}_3$ , and  $\text{TiO}_2$ , the solution of oxidant 0.27 g of  $\text{FeCl}_3$  (dissolved in 10 mL  $\text{H}_2\text{O}$ ) was added. A greenish-black color indicated the start of the polymerization process and the reaction was left to occur for 6 h. The resulting composite was thereafter filtered and washed with an excess of water, ethanol, and acetone to remove the PPy oligomers, unreacted oxidant, and other impurities. The prepared

Ag/TiO<sub>2</sub>@PPy nanocomposite was dried in an air oven for 24 h at 80 °C and stored in a desiccator for its further use. A TiO<sub>2</sub>@PPy nanocomposite was also prepared similarly in the absence of AgNO<sub>3</sub>.

### 3.3. Characterization

The morphology of Ag/TiO<sub>2</sub>@PPy was studied by field emission scanning electron microscopy (FESEM) (JSM-7500 F; JEOL, Tokyo, Japan) and transmission electron microscopy (TEM) (model Tecnai G2 F20 Super Twin) at 200 kV with LaB<sub>6</sub> emitter. The UV-vis spectra of Ag/TiO<sub>2</sub>, TiO<sub>2</sub>@PPy and Ag/TiO<sub>2</sub>@PPy were recorded with a Perkin Elmer UV-visible diffuse reflectance spectrophotometer in the range of 200–900 nm. X-ray photoelectron spectroscopy (XPS) measurements were recorded on a SPECS GmbH, (Berlin, Germany) spectrometer using a non-monochromatic Mg-K $\alpha$  (1253.6 eV). X-ray source. X-ray diffraction (XRD) spectra of Ag/TiO<sub>2</sub> and Ag/TiO<sub>2</sub>@PPy were recorded by an Ultima-IV (Rigaku, Japan) diffractometer using Cu K $\alpha$  radiation.

### 3.4. Photocatalytic Activity

The photocatalytic degradation of MB under ultraviolet-C and visible light irradiation (112 W) was conducted in a 200-mL Pyrex beaker containing 100 mL dye solution under continuous aeration and magnetic stirring. The photocatalytic reactions at a fixed photocatalyst mass (0.1 g) were performed by varying the operational conditions such as solution pH (from 3 to 9), reaction time (between 5 and 180 min), and initial MB concentration (from 4 to 20 mg/L). Before starting the photocatalytic reactions, the solutions were kept in the dark for 30 min for the adsorption MB onto the materials and then the solutions were illuminated with UV/visible light. After photocatalytic reaction, the solutions were filtered through a 0.22- $\mu$ m syringe filter and the amount of MB remaining in the supernatant solution was determined at a maximum wavelength of 665 nm using a HACH LANGE DR-6000 UV-visible spectrometer.

## 4. Conclusions

Ag/TiO<sub>2</sub>, TiO<sub>2</sub>@PPy, and Ag/TiO<sub>2</sub>@PPy nanocomposites were successfully synthesized. XPS studies indicated that Ag was present in metallic and ionic forms. The UV-visible absorption studies showed that all the synthesized composites are effective visible light sensitizers. Ag/TiO<sub>2</sub>@PPy showed superior photocatalytic activity in comparison to Ag/TiO<sub>2</sub> and TiO<sub>2</sub>@PPy under UV and visible light. The superior photocatalytic activity of Ag/TiO<sub>2</sub>@PPy heterojunction may be due to the higher e<sup>-</sup>/h<sup>+</sup> charge separation (there is a built-in electrostatic field at the heterojunction). PPy plays the role of photosensitizer and electron acceptor in order to enhance the photodecomposition of MB in aquatic solution. The maximum photocatalytic activity of Ag/TiO<sub>2</sub>@PPy for MB was observed at pH 9 and the pseudo-first order rate constant values were 0.044 and 0.003 min<sup>-1</sup> under UV and visible light irradiation, respectively. The effect of initial dye concentration revealed that the degradation of MB decreased from 100% to 18.85% under UV light and from 100% to 83% in visible light when the MB concentration increased from 4 to 20 mg·L<sup>-1</sup>. These results suggest that Ag/TiO<sub>2</sub>@PPy could be used as a promising material for the application of organic pollutant photodegradation in a vast variety of areas.

**Acknowledgments:** This project was supported by the NSTIP strategic technologies program in the Kingdom of Saudi Arabia – Project No (11-ENE1531-03). The authors also, acknowledge with thanks Science and Technology Unit, King Abdulaziz University for technical support.

**Author Contributions:** Mohamed A Barakat and Reda M. El-Shishtawy designed this work. Reda M. El-Shishtawy synthesized the materials. Rajeev Kumar conducted the experimental work and the manuscript was written by Rajeev Kumar and Mohamed A. Barakat.

**Conflicts of Interest:** The authors declare no conflict of interest.

## References

1. Curti, M.; Bahnemann, D.W.; Mendive, C.B. Mechanisms in Heterogeneous photocatalysis. In *Reference Module in Materials Science and Materials Engineering*; Elsevier: Amsterdam, The Netherlands, 2016. [CrossRef]
2. Paez, C.A.; Poelman, D.; Pirard, J.P.; Heinrichs, B. Unpredictable photocatalytic ability of H<sub>2</sub>-reduced rutile-TiO<sub>2</sub> xerogel in the degradation of dye-pollutants under UV and visible light irradiation. *Appl. Catal. B* **2010**, *94*, 263–271. [CrossRef]
3. Liua, X.; Zhanga, H.; Liu, C.; Chen, J.; Li, G.; An, T.; Wong, P.K.; Zhao, H. UV and visible light photoelectrocatalytic bactericidal performance of 100% {111} faceted rutile TiO<sub>2</sub> photoanode. *Catal. Today* **2014**, *224*, 77–82. [CrossRef]
4. McEvoy, J.G.; Cui, W.; Zhang, Z. Degradative and disinfective properties of carbon-doped anatase-rutile TiO<sub>2</sub> mixtures under visible light irradiation. *Catal. Today* **2013**, *207*, 191–199. [CrossRef]
5. Egerton, T.A.; Purnama, H.; Mattinson, J.A. The influence of platinum (II) on TiO<sub>2</sub> photocatalyzed dye decolourization by rutile, P25 and PC500. *J. Photochem. Photobiol. A* **2011**, *224*, 31–37. [CrossRef]
6. Dolat, D.; Ohtani, B.; Mozia, S.; Moszynski, D.; Guskos, N.; Bieluna, Z.L.; Morawski, A.W. Preparation, characterization and charge transfer studies of nickel—Modified and nickel, nitrogen co-modified rutile titanium dioxide for photocatalytic application. *Chem. Eng. J.* **2014**, *239*, 149–159. [CrossRef]
7. Dolat, D.; Mozia, S.; Ohtani, B.; Morawski, A.W. Nitrogen, Iron-single modified (N-TiO<sub>2</sub>, Fe-TiO<sub>2</sub>) and co-modified (Fe, N-TiO<sub>2</sub>) rutile titanium dioxide as visible-light active photocatalysts. *Chem. Eng. J.* **2013**, *225*, 358–364. [CrossRef]
8. Ansari, M.O.; Khan, M.M.; Ansari, S.A.; Raju, K.; Lee, J.; Cho, M.H. Enhanced thermal stability under DC electrical conductivity retention and visible light activity of Ag/TiO<sub>2</sub>@polyaniline nanocomposite film. *ACS Appl. Mater. Interfaces* **2014**, *6*, 8124–8133. [CrossRef] [PubMed]
9. Yang, Y.; Wen, J.; Wei, J.; Xiong, R.; Shi, J.; Pan, C. Polypyrrole-decorated Ag-TiO<sub>2</sub> nanofibers exhibiting enhanced photocatalytic activity under visible-light illumination. *ACS Appl. Mater. Interfaces* **2013**, *5*, 6201–6207. [CrossRef] [PubMed]
10. Wang, X.; Li, S.; Yu, H.; Yu, J.; Liu, S. Ag<sub>2</sub>O as a new visible-light photocatalyst: Self-stability and high photocatalytic activity. *Chem. Eur. J.* **2011**, *17*, 7777–7780. [CrossRef] [PubMed]
11. Zhou, W.J.; Leng, Y.H.; Hou, D.M.; Li, H.D.; Li, L.G.; Li, G.Q.; Liu, H.; Chen, S.W. Phase transformation and enhanced photocatalytic activity of S-Doped Ag<sub>2</sub>O/TiO<sub>2</sub> heterostructured nanobelts. *Nanoscale* **2014**, *6*, 4698–4704. [CrossRef] [PubMed]
12. Duana, F.; Zhanga, Q.; Shi, D.; Chen, M. Enhanced visible light photocatalytic activity of Bi<sub>2</sub>WO<sub>6</sub> via modification with polypyrrole. *Appl. Surf. Sci.* **2013**, *268*, 129–135. [CrossRef]
13. Upadhyay, R.K.; Sooin, N.; Roy, S.S. Role of graphene/metal oxide composites as photocatalysts, adsorbents and disinfectants in water treatment. *RSC Adv.* **2014**, *4*, 3823–3851. [CrossRef]
14. Deng, F.; Li, Y.; Luo, X.; Yang, L.; Tu, X. Preparation of conductive polypyrrole/TiO<sub>2</sub> nanocomposite via surface molecular imprinting technique and its photocatalytic activity under simulated solar light irradiation. *Coll. Surf. A* **2012**, *395*, 183–189. [CrossRef]
15. Haspulat, B.; Gülce, A.; Gülce, H. Efficient photocatalytic decolorization of some textile dyes using Fe ions doped polyaniline film on ito coated glass substrate. *J. Hazard. Mater.* **2013**, *260*, 518–526. [CrossRef] [PubMed]
16. Zhang, Z.; Yuan, Y.; Liang, L.; Cheng, Y.; Xu, H.; Shi, G.; Jin, L. Preparation and photoelectrochemical properties of a hybrid electrode composed of polypyrrole encapsulated in highly ordered titanium dioxide nanotube Array. *Thin Solid Films* **2008**, *516*, 8663–8667. [CrossRef]
17. Tan, Y.; Chen, Y.; Mahimwalla, Z.; Johnson, M.B.; Sharma, T.; Brüning, R.; Ghandi, K. Novel synthesis of rutile titanium dioxide–polypyrrole nano composites and their application in hydrogen generation. *Synth. Met.* **2014**, *189*, 77–85. [CrossRef]
18. Gu, S.; Li, B.; Zhao, C.; Xu, Y.; Qian, X.; Chen, G. Preparation and characterization of visible light-driven AgCl/PPy photocatalyst. *J. Alloys Comp.* **2011**, *509*, 5677–5682. [CrossRef]
19. Wang, B.; Li, C.; Pang, J.; Qing, X.; Zhai, J.; Li, Q. Novel Polypyrrole-Sensitized Hollow TiO<sub>2</sub>/Fly Ash Cenospheres: Synthesis, characterization, and photocatalytic ability under visible light. *Appl. Surf. Sci.* **2012**, *258*, 9989–9996. [CrossRef]

20. Kandiel, T.A.; Dillert, R.D.; Bahnemann, D.W. Enhanced photocatalytic production of molecular hydrogen on TiO<sub>2</sub> modified with Pt-polypyrrole nanocomposites. *Photochem. Photobiol. Sci.* **2009**, *8*, 683–690. [[CrossRef](#)] [[PubMed](#)]
21. Ren, H.T.; Jia, S.Y.; Wu, Y.; Wu, S.H.; Zhang, T.H.; Han, X. Improved photochemical reactivities of Ag<sub>2</sub>O/gC<sub>3</sub>N<sub>4</sub> in phenol degradation under UV and visible light. *Ind. Eng. Chem. Res.* **2014**, *53*, 17645–17653. [[CrossRef](#)]
22. Kowal, K.; Kopaczynska, K.W.K.M.; Dworniczek, E.; Franciczek, R.; Wawrzynska, M.; Vargova, M.; Zahoran, M.; Rakovsky, E.; Kus, P.; Plesch, G.; *et al.* In-situ photoexcitation of silver-doped titania nanopowders for activity against bacteria and yeasts. *J. Colloid Interface Sci.* **2011**, *362*, 50–57. [[CrossRef](#)] [[PubMed](#)]
23. Liang, N.; Wang, M.; Jin, L.; Huang, S.; Chen, W.; Xu, M.; He, Q.; Zai, J.; Fang, N.; Qian, X. Highly efficient Ag<sub>2</sub>O/Bi<sub>2</sub>O<sub>2</sub>CO<sub>3</sub> p-n heterojunction photocatalysts with improved visible-light responsive activity. *ACS Appl. Mater. Interfaces* **2014**, *6*, 11698–11705. [[CrossRef](#)] [[PubMed](#)]
24. Qiao, Y.; Shen, L.; Wu, M.; Guo, Y.; Meng, Y. A novel chemical synthesis of bowl-shaped polypyrrole particles. *Mater. Lett.* **2014**, *126*, 185–188. [[CrossRef](#)]
25. Kang, E.T.; Neoh, K.G.; Ong, Y.K.; Tan, K.L.; Tan, B.T.G. XPS studies of proton modification and some anion exchange processes in polypyrrole. *Synth. Met.* **1990**, *30*, 69–80. [[CrossRef](#)]
26. Landureau, E.P.; Nicolau, Y.F.; Delamar, M. XPS study of layer-by-layer deposited polypyrrole thin films. *Synth. Met.* **1995**, *72*, 111–119. [[CrossRef](#)]
27. Ansari, M.O.; Yadav, S.K.; Cho, J.W.; Mohammad, F. Thermal stability in terms of DC electrical conductivity retention and the efficacy of mixing technique in the preparation of nanocomposites of graphene/polyaniline over the carbon nanotubes/polyaniline. *Compos. Part B* **2013**, *47*, 155–161. [[CrossRef](#)]
28. Pérez-Bustamante, R.; Pérez-Bustamante, F.; Estrada-Guel, I.; Santillán-Rodríguez, C.R.; Matutes-Aquino, J.A.; Herrera-Ramírez, J.M.; Miki-Yoshida, M.; Martínez-Sánchez, R. Characterization of Al<sub>2024</sub>-CNTs composites produced by mechanical alloying. *Powder Technol.* **2011**, *212*, 390–396. [[CrossRef](#)]
29. Zhou, W.; Liu, H.; Wang, J.; Liu, D.; Du, G.; Cui, J. Ag<sub>2</sub>O/TiO<sub>2</sub> nanobelts heterostructure with enhanced ultraviolet and visible photocatalytic activity. *ACS Appl. Mater. Interfaces* **2010**, *8*, 2385–2392. [[CrossRef](#)] [[PubMed](#)]
30. Wang, Y.; Liu, L.; Xu, L.; Cao, X.; Li, X.; Huang, Y.; Meng, C.; Wang, Z.; Zhu, W. Ag<sub>2</sub>O/TiO<sub>2</sub>/V<sub>2</sub>O<sub>5</sub> one-dimensional nanoheterostructures for superior solar light photocatalytic activity. *Nanoscale* **2014**, *6*, 6790–6797. [[CrossRef](#)] [[PubMed](#)]
31. Zhang, X.; Bai, R. Surface electric properties of polypyrrole in aqueous solutions. *Langmuir* **2003**, *19*, 10703–10709. [[CrossRef](#)]
32. Bhaumik, M.; McCrindle, R.; Maity, A. Efficient removal of Congo red from aqueous solutions by adsorption onto interconnected polypyrrole-polyaniline nanofibres. *Chem. Eng. J.* **2013**, *228*, 506–515. [[CrossRef](#)]
33. Li, J.; Feng, J.; Yan, W. Excellent adsorption and desorption characteristics of polypyrrole/TiO<sub>2</sub> composite for methylene blue. *Appl. Surf. Sci.* **2013**, *279*, 400–408. [[CrossRef](#)]
34. Moziaa, S.; Morawski, A.W.; Toyoda, M.; Tsumura, T. Effect of process parameters on photodegradation of acid yellow 36 in a hybrid photocatalysis-membrane distillation system. *Chem. Eng. J.* **2009**, *150*, 152–159. [[CrossRef](#)]
35. Reuterglrdh, L.B.; Iangphasuk, M. Photocatalytic decolourization of reactive azo dye: A comparison between TiO<sub>2</sub> and CdS photocatalysis. *Chemosphere* **1997**, *35*, 585–596. [[CrossRef](#)]
36. Zhang, H.; Zhong, X.; Xu, J.J.; Chen, H.Y. Fe<sub>3</sub>O<sub>4</sub>/Polypyrrole/Au nanocomposites with core/shell/shell structure: Synthesis, characterization, and their electrochemical properties. *Langmuir* **2008**, *24*, 13748–13752. [[CrossRef](#)] [[PubMed](#)]
37. Sarkar, D.; Ghosh, C.K.; Mukherjee, S.; Chattopadhyay, K.K. Three dimensional Ag<sub>2</sub>O/TiO<sub>2</sub> type-II (p-n) nanoheterojunctions for superior photocatalytic activity. *ACS Appl. Mater. Interfaces* **2013**, *5*, 331–337. [[CrossRef](#)] [[PubMed](#)]

